Complexation of a polyelectrolyte with oppositely charged spherical macroions: Giant inversion of charge

Toan T. Nguyen and Boris I. Shklovskii
Department of Physics, University of Minnesota, 116 Church Street Southeast, Minneapolis, Minnesota 55455

(Received 14 November 2000; accepted 22 January 2001)

Complexation of a long flexible polyelectrolyte (PE) molecule with oppositely charged spherical particles such as colloids, micelles, or globular proteins in a salty water solution is studied. PE binds spheres winding around them, while spheres repel each other and form almost periodic necklace. If the total charge of PE in the solution is larger than total charge of spheres, repulsive correlations of PE turns on a sphere lead to inversion of the net charge of each sphere. In the opposite case when the total charge of spheres is larger, we predict another correlation effect; spheres bind to the PE in such a great number that they invert the charge of the PE. The inverted charge by absolute value can be larger than the bare charge of PE even when screening by monovalent salt is weak. At larger concentrations of monovalent salt, the inverted charge can reach giant proportions. Near the isoelectric point where total charges of spheres and PE are equal, necklaces condense into macroscopic bundles. Our theory is in qualitative agreement with recent experiments on micelles–PE systems. © *2001 American Institute of Physics.* [DOI: 10.1063/1.1355289]

I. INTRODUCTION

Electrostatic interactions play an important role in aqueous solutions of biological and synthetic polyelectrolytes (PE). The complexation of a long flexible polyelectrolyte with oppositely charged spherical particles such as micelles,[1] globular proteins[2] or colloids[3] is a generic electrostatic problem of the polymer physics. A long PE binds oppositely charged spheres winding around each of them (Fig. 1). Without losing the generality, we assume that the PE is negative and spheres are positive.

If the charge of a sphere is not completely compensated by the winding PE, the net charge of the sphere is still positive, and the neighboring spheres repel each other and form on the PE an almost periodic necklace (Fig. 1). The same picture is true when the winding PE inverts the net charge of each sphere making it negative. We call this nontrivial phenomenon a sphere charge inversion (SCI). SCI is known to happen in the most famous biological example of PE-spheres complexation. In the chromatin, the negative double-helix DNA molecule winds around a positive histone octamer to form a complex known as the nucleosome bead. Nucleosome beads are connected by DNA linkers in the so-called beads-on-a-string structure. When linkers are cut enzymatically each nucleosome bead is found to have a negative net charge.

The counterintuitive phenomenon of SCI has attracted a lot of attention of theorists. However, all theoretical and numerical studies of SCI, have been done for the complexation a single sphere with a PE molecule.[4–10]

In this paper, we propose the first theory of the SCI in the necklacelike complex of the PE with many spheres. Our theory accounts for the interaction between different spheres. We argue that in this case, as in the case of a single sphere,[10] SCI happens due to repulsive correlations of different turns of the PE on the surface of spheres.

For many spheres, however, not only the net charge of a sphere should be found, but simultaneously the number of spheres attached to PE molecules is to be calculated. Therefore, the second and even more challenging problem is to determine the sign of the whole complex of the PE with many spheres. Is it positive or negative at given number concentrations of PE, n_p, and spheres, n_s, in solution?

The standard Debye–Hückel and Poisson–Boltzmann theories of screening of the PE by monovalent counterions leave the net charge of the PE always negative. These theories, however, do not work for screening by strongly charged spheres which, as we mentioned above, form a correlated sequence, reminding a necklace or a one-dimensional Wigner crystal. One can call it a Wigner liquid, because the long range order in many practical situations is destroyed.

Wigner-crystal-like correlations between multivalent counterions are known to lead to charge inversion of rigid macroions.[10–15,7] This happens because when a multivalent ion approaches an already neutralized macroion, it repels other counterions, creates for itself a correlation hole or an image of opposite charge which attracts it to the surface. In the necklace shown above, the PE segment wound around each sphere interacts exclusively with this sphere and plays the role of the correlation hole or a Wigner–Seitz cell. Therefore, again, Wigner-crystal-like correlations come into play and lead to an additional attraction of the spheres to the PE. Indeed, when a new sphere approaches a neutralized necklace, it pushes other spheres away, unwinds a segment of PE from them and winds this segment around itself. This segment is the sphere's correlation hole or, in other words, its image in the PE. We are dealing with the correlation physics because the image appears only in response to the

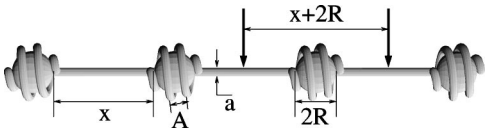

FIG. 1. The beads-on-a-string complex of a negative PE molecule and many positive spheres. On the surface of each sphere, due to the Coulomb repulsion, neighboring PE turns lie parallel to each other. Locally, they resemble an one-dimensional Wigner crystal with the lattice constant A. At a larger scale, charged spheres repel each other and form another one-dimensional Wigner crystal along the PE with lattice constant $x+2R$. A Wigner–Seitz cell of this crystal is shown by the thick arrows.

new sphere. We show below that, at large n_s and small n_p, this correlation attraction leads to PE charge inversion (PECI). PECI was observed in a micelle–PE system.[1]

Following Refs. 11–13 for a quantitative characteristic of charge inversion we introduce the charge inversion ratio of the PE, $\mathcal{P}=-Q^*/Q$, where $Q=L\eta$ is the negative bare charge of the PE (L and η are, respectively, the contour length and the linear charge density of a PE molecule) and Q^* is its positive net charge together with all adsorbed spheres. Optimization of the free energy of a complex with respect of the number of bound spheres per PE molecule, N, shows that, even for a large Debye–Hückel screening radius r_D of the solution, the optimal $N=N_0$ is so large that

$$\mathcal{P}=\left(\frac{q}{R\eta\alpha}\right)^{1/4}\gg 1. \tag{1}$$

Here R and q is the radius and charge of a sphere and α is a dimensionless logarithmic function of $qR/\eta r_D^2$ (see Sec. III). We assume everywhere in this paper that $q/\eta R\gg 1$, so that more than one turn of PE winds around the sphere to neutralize it.

PECI also grows with stronger screening (smaller r_D). For r_D in the range $A\ll r_D\ll R(q/R\eta)^{1/2}$, we show that

$$\mathcal{P}=\sqrt{\frac{q}{r_D\eta\beta}}\gg\left(\frac{q}{R\eta}\right)^{1/4}\gg 1. \tag{2}$$

Here β is a dimensionless function of $q/R\eta$ and R/r_D (see Sec. V). A PECI given by Eq. (1) and Eq. (2) can be called giant.

At a large sphere concentration n_s, when the PE number concentration, n_p, grows and reaches n_s/N_0, the pool of free spheres gets exhausted and each PE molecule cannot get the optimal number N_0 of them any more. Then the PECI becomes weaker and disappears linearly at the isoelectric point $n_{pi}=qn_s/|Q|$, where the total charge of all the spheres compensates for the total charge of all PE molecules. When the concentration n_p continues to grow beyond n_{pi} practically all the spheres remain bound to the PE and the net charge Q^* is negative and grows by absolute value. The variation of Q^*/Q with n_p is shown in Fig. 2 by the solid line.

Simultaneously with these variations of Q^*/Q, the net charge q^* of a sphere changes, too. At $n_p<n_s/N_0$ it is positive and close to q. At $n_p>n_s/N_0$, the net charge q^* starts to decrease linearly with n_p-n_{pi}. At the isoelectric point

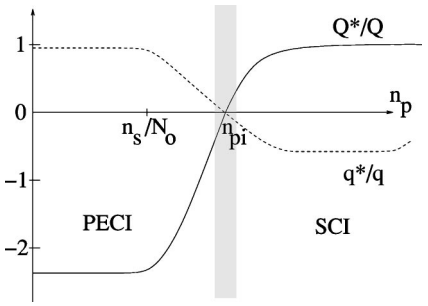

FIG. 2. Schematic plot of q^*/q and Q^*/Q as functions of the PE concentration, n_p, at a fixed and large sphere concentration n_s and at a not very large r_D. The shaded stripe corresponds to the region around the isoelectric point $n_p=n_{pi}$ where necklaces condense into macroscopic bundles.

$n_p=n_{pi}$, the charge q^* crosses zero and simultaneously, the linker length x vanishes. At $n_p>n_{pi}$, the charge q^* becomes negative and SCI appears. We show that the charge inversion ratio of a sphere, $\mathcal{S}=-q^*/q$, grows with n_p-n_{pi} until it reaches the value corresponding to a single sphere bound to infinite PE,[10] which is roughly equal to the inverse number of turns necessary for PE to neutralize a sphere. The behavior of q^*/q as function of n_p is shown by dashed line in Fig. 2. It is clear from Fig. 2 that SCI happens at $n_p>n_{pi}$ and PECI at $n_p<n_{pi}$.

Thus, we arrive at the conclusion that both at $n_p>n_{pi}$ and $n_P<n_{pi}$, a beads-on-a-string structure can spontaneously self-assemble from a PE and oppositely charged spheres without any non-Coulomb forces. The latter structure resembles the 10 nm fiber structure of the chromatin.

Experimental observation of SCI is possible when spheres with winding PE are cut out from the complex. Then their charge can be measured by electrophoresis.

Consequences of PECI are more pronounced. PECI leads to reentrant condensation of necklaces into macroscopic bundles. Indeed, near the isoelectric point $n_p=n_{pi}$ each complex is almost neutral and short range attractive forces between Wigner-crystal-like complexes[16] lead to their condensation and coacervation. Away from the isoelectric point each necklace complex is charged and their long range repulsive interactions prevent their condensation. One can watch how condensation begins and ends changing one of concentrations. For example, if we keep the spheres concentration n_s large and fixed and start from $n_p\gg n_{pi}$, the complexes are negative and repel each other. Then with decreasing n_p the condensation happens in the vicinity of the isoelectric point (the shaded region in Fig. 2). If we continue decreasing n_p, PECI begins and the complexes become positive. When their positive charge, Q^*, becomes large enough, the coaservate dissolves. An important prediction of such theory[17] is that the electrophoretic mobility changes sign in the coaservation range. We estimate the width of the range of n_p around n_{pi} where coaservation occurs. This width increases with decreasing r_D and at $r_D\ll A$,

$$\frac{\delta n_p}{n_{pi}}=\left(\frac{R\eta}{q}\right)^2\frac{R}{r_D}. \tag{3}$$

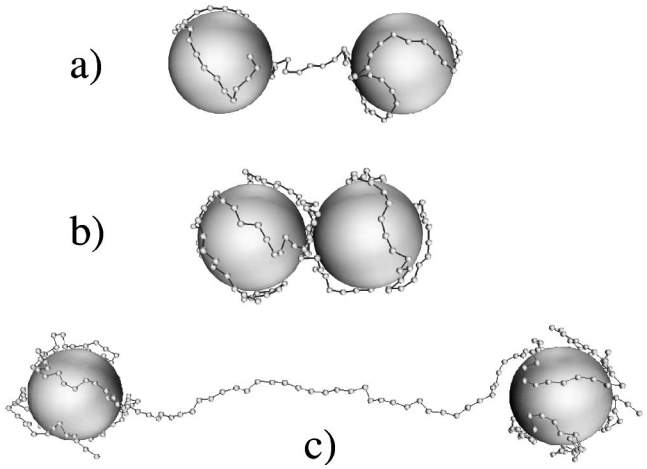

FIG. 3. Snapshots of three complexes of a negative PE with two positively charged spheres. The numbers of monomers of the PE in the cases (a), (b), and (c) are 70, 140, and 210, respectively. All the spheres have charge $70e$. The total charges of the complexes are $70e$, 0, and $-70e$, respectively.

The narrow range of coaservation followed by resolubilization was observed in the micelles–PE system[1] as a function of the charge of micelles. The electrophoretic mobility of complexes was indeed found to change sign within the interval of the micelle charge in which coaservation happens. The width of the coaservation region was also observed to increase with decreasing r_D in qualitative agreement with Eq. (3).

To illustrate the physical picture discussed above we carry out Monte Carlo simulation of the complexation of a negative PE with two positively charged spheres. The system is in a salt-free solution. The simulated spheres have charge $70e$ uniformly distributed over their surface and radius $3.5l_B$, where $l_B=7.2$ Å is the Bjerrum length at the room temperature. The PE is modeled as a chain of free jointed hard spherical beads with radius $0.2l_B$ and charge $-e$. The bond length is kept fixed and equal l_B. The Monte Carlo algorithm is described in our previous paper (Ref. 10).

The snapshots of three such complexes are shown in Fig. 3. In the first simulation, the PE molecule has 70 monomers. This complex illustrates the regime where the spheres are in abundance ($n_p<n_s/N_0$). In the second simulation, the PE molecule has 140 monomers so that the complex is neutral and illustrates the PE-spheres complexes near the isoelectric point $n_p=n_{pi}$. In the last simulation, the PE molecule has 210 monomers. This complex illustrates the regime where there are not enough spheres to neutralize the PE ($n_p>n_{pi}$). PECI is clearly observed in the first simulation. One PE with charge $-70e$ complexes with the two spheres with charge $70e$ each, making a giant 100% PECI. Around the isoelectric point, the distance between the surfaces of the two spheres is practically zero (less than the length of one PE bond l_B). Many such PE-spheres complexes condense into a large bundle around the isoelectric point. Far beyond the isoelectric point, the PE-spheres complex is stretched again. SCI is observed with around 85 PE monomers bound to each sphere ($\sim$20% SCI).

Although a perfect solenoid conformation of PE is not observed in Fig. 3, one can clearly see that PE segments of different turns stay away from each other and locally resemble a one-dimensional Wigner crystal which helps to lower the energy of the system. Globally, thermally excited soft bending modes with characteristic length R melt the solenoid into a compromised ''tennis ball'' conformation.[10] The difference in energy between a ''tennis ball'' and a solenoid, however, is small compare to the interaction between the spheres and the PE. This explains the agreement between the observed physical features of the simulated finite temperature systems and those predicted by our zero temperature theory.

Here, we also would like to mention recent Monte Carlo simulations[18] of complexation of a PE molecule of given length with many oppositely charged spheres. Results of this work are in qualitative agreement with Fig. 2. However, we cannot compare them with our theory quantitatively because in these simulations the parameter $q/R\eta$ is not large.

It should also be noted that the behavior of charge inversion for PE-spheres complexes described above is qualitatively similar to that of lipid-DNA complexes studied in Refs. 19 and 20 where one sees both kinds of charge inversion as one moves away from the isoelectric point.

This paper is organized as follows: In Sec. II, we study the free energy of the system and derive equations for the equilibrium values of x and N. In Secs. III and IV, these equations are solved for the weak screening case where the screening radius r_D is larger than the necklace period $x+2R$. In Sec. V, we discuss condensation and resolubilization near the isoelectric point. Section VI is devoted to the strong screening case, $r_D \ll x+2R$. We show that in this case PECI is much stronger. In Sec. VII, we derive the charge inversion ratio for a stiff (rodlike) PE and compare it to the result for an intrinsically flexible PE obtained in previous sections. It is shown that at weak screening, PECI is stronger for flexible PE while at strong screening, PECI is stronger for rigid PE. This means that if one stretches the PE by external force, some spheres leave the PE in the weak screening case and condense on the PE in the strong screening case. Finally, in the conclusion, we discuss several important assumptions used in this work.

II. OPTIMIZATION OF THE COMPLEX STRUCTURE: WEAK SCREENING CASE

Let us start by writing down the free energy of the complex of a PE with length L and charge density η winding consequently around N oppositely charged spheres of charge q and radius R (see Fig. 1). First, we assume the complex is in a low salt solution so that the screening radius r_D is larger than the distance between two neighboring spheres $x+2R$. We call this situation the weak screening case. Taking into account that the length of the PE segment that winds around each sphere is $(L/N-x)$, we have

$$F(N,x)=\frac{Q^{*2}}{DN(x+2R)}\ln\mathcal{N}+Nf(x), \tag{4}$$

where

$$f(x)=\frac{q^{*2}}{2RD}-\frac{2q^*\eta}{D}\ln\frac{x+2R}{2R}+(x+2R)\frac{\eta^2}{D}\ln\frac{x+2R}{2R}-(x+4R)\frac{\eta^2}{D}\ln\frac{x+4R}{4R}+(L/N-x)\frac{\eta^2}{D}\ln\frac{A}{a}+x\frac{\eta^2}{D}\ln\frac{x}{2a}. \quad (5)$$

Here D is the dielectric constant of water. At a length scale greater than its period $x+2R$, the complex is a uniform rod of length $N(x+2R)$ and charge density $Q^*/N(x+2R)$. The first term in Eq. (4) is the self-energy of this necklace (the macroscopic self-energy). The logarithmic divergence of this energy is cut off at small distances by $x+2R$ and at large distances by the length

$$\mathcal{N}(x+2R)=\min\{r_D,N(x+2R)\}, \quad (6)$$

where $N(x+2R)$ is the rod length. In the second term of Eq. (4), $f(x)$ accounts for the total energy of one period of the necklace. It is calculated as the energy of a Wigner–Seitz cell consisting of a sphere with two PE tails of length $x/2$. The first terms in Eq. (5) accounts for the self-energy of the adsorbed sphere with net charge q^* at the PE. The second term accounts for the interaction of the sphere with the tails, the third and fourth terms account for the interaction between the tails. The fifth and sixth terms are, respectively, the self-energies of the PE wound around the macroion (which is screened at distance A between turns) and of the two straight tails with length $x/2$. It should be noted that writing down the second of Eq. (4) as $Nf(x)$ we have neglected the difference between the end spheres with those in the middle of the PE. This is justified for a reasonably large value of N. It should also be noted that we neglected the entropy of the PE monomers in the tails and at the spheres surface. This is justified because the charge of the sphere is large and Coulomb energy is much larger than the thermal energy of PE.

As we will see later, when n_p is away from the isoelectric point n_{pi}, the linker length x is much larger than R. This helps to simplify Eqs. (4) and (5). Approximating $A\simeq R^2/(L/N-x)$ and keeping only terms of the highest order in the large parameter x/R, one can rewrite these equations as

$$F(N,x)=\frac{\delta^2}{x}N\ln\mathcal{N}+Nf(x) \quad (7)$$

$$f(x)=\frac{(\delta+x)^2}{2R}-2(\delta+x)\ln\frac{x}{R}-(L/N-x)\ln\frac{(L/N-x)a}{R^2}+x\ln\frac{x}{a}, \quad (8)$$

where we introduce the PE length needed to neutralize one sphere $\mathcal{L}=q/\eta$ and

$$\delta=\mathcal{L}-L/N=Q^*/N\eta, \quad (9)$$

so that $q^*=\eta(\delta+x)$. From now on, we also write the energy in units of η^2/D (hence, the energy has dimensionality of length).

At a given N, the optimal distance x can be calculated by minimizing the free energy $F(N,x)$ with respect to x. This gives, to the leading terms,

$$\frac{\partial F}{\partial x}=-\frac{\delta^2}{x^2}\ln\mathcal{N}+\frac{\delta+x}{R}-\ln\frac{x}{R}+\ln\frac{L/N-x}{R}=0. \quad (10)$$

The physical meaning of each term in Eq. (10) is quite clear. When one brings a unit length of the PE from the sphere surface to their tails, thereby increasing x, the four terms of Eq. (10) are, respectively, the lowering in the system's macroscopic energy (with increasing x), the potential energy cost due to the attraction of the PE to the sphere, the potential energy gained due to the repulsion of two PE tails of each sphere and finally the cost in the correlation energy at the surface of the sphere. This last term—the correlation energy term—needs further clarification. If the PE turns around a sphere were randomly oriented, its self-energy per unit length would be $\ln(R/a)$. In reality, due to strong lateral repulsion between different PE turns, they lie parallel to each other and locally resemble a one-dimension Wigner crystal. In this ordered state, the self-energy per unit length of the PE turn is screened at distance A instead of R. This gives the energy $\ln(A/a)$ per unit length of the PE. The lowering in the self-energy of the PE segment wound around a sphere (with length $(L/N-x)$) in the ordered state as compared to the randomly oriented state is equal to $(L/N-x)[\ln(R/a)-\ln(A/a)]=(L/N-x)\ln(R/A)\simeq(L/N-x)\ln((L/N-x)/R)$ and is called the correlation energy. The fourth term of Eq. (10) is its derivative with respect of x. A more detail discussion of this correlation effect can be found in Ref. 10.

In principle, one can solve Eq. (10) numerically for x as a function of N and other parameters of the system L/R and $\mathcal{L}/R$. After that, one can substitute $x(N)$ back into Eq. (7) and find the optimal value N_0 from the equation,

$$\left.\frac{dF(N,x(N))}{dN}\right|_{N=N_0}=\mu_s, \quad (11)$$

where μ_s is the chemical potential of spheres in the solution.

If the PE concentration is small ($n_p<n_s/N_0$) then N_0 and $x(N_0)$ define the configuration of the complex. However, in the case $n_p>n_s/N_0$ there are less than N_0 spheres for each PE. In this case, $N=n_s/n_p$ (with an exponentially small correction) and $x(N)$ defines the configuration of the complex.

Let us now study asymptotic limits in which Eq. (10) can be solved analytically providing clear physical picture of our system.

III. A SINGLE POLYELECTROLYTE MOLECULE IN CONCENTRATED SOLUTION OF SPHERES: WEAK SCREENING CASE

In this section we consider the case where the PE concentration is small, $n_p<n_s/N_0$, so that the optimization of $F(N,x(N))$ with respect to N is needed to get the optimal configuration of the complex. Here and everywhere in this paper we assume the sphere concentration is high enough so

that one can approximate $\mu_s = \mathcal{L}^2/2R$ (the self-energy of a bare sphere) neglecting the entropic part of the chemical potential. Equation (11) can be rewritten as

$$\frac{\mathcal{L}^2}{2R} = \frac{dF}{dN} = \frac{\delta^2}{x}\left(1 + \frac{2L}{N\delta} - \frac{Nx'}{x}\right)\ln\mathcal{N} + \frac{(\delta+x)^2}{2R}\left(1 + \frac{2L}{N(\delta+x)} + \frac{2Nx'}{\delta+x}\right) - (2\mathcal{L} + x + Nx')\ln\frac{x}{2R} + (x+Nx')\ln\frac{L/N-x}{R}, \tag{12}$$

where $x' = dx/dN$.

To solve Eq. (10) for x, we assume that $\mathcal{L} \gg R\ln\mathcal{N}$ or, in other words, the screening length is smaller than an exponentially large length, $r_D \ll x\exp(\mathcal{L}/R)$. As we see below, in this case $\delta \gg x$ and the last two terms in Eq. (10) can be neglected. This gives

$$x = \delta^{1/2}(R\ln\mathcal{N})^{1/2}. \tag{13}$$

Substituting Eq. (13) into Eq. (12) and keeping only the highest order terms one obtains the equation

$$(\delta R\ln\mathcal{N})^{1/2}(2\delta + 3L/N) - (L/N)^2/2 = 0, \tag{14}$$

which has consistent solution only if $\delta \gg L/N$. In this case,

$$\delta \sim \frac{L}{N}\left(\frac{L/N}{R\ln\mathcal{N}}\right)^{1/3}, \tag{15}$$

and the solution for $N_0 = L/(x+2R)$ is

$$N_0 = \frac{L}{\delta^{3/4}(R\ln\mathcal{N})^{1/4}} \simeq \frac{L}{\mathcal{L}^{3/4}(R\ln\mathcal{N})^{1/4}}. \tag{16}$$

The corresponding charge inversion ratio is

$$\mathcal{P} = -\frac{Q^*}{Q} = \frac{N_0\delta}{L} = \left(\frac{\mathcal{L}}{R\ln\mathcal{N}}\right)^{1/4} \gg 1. \tag{17}$$

From Eqs. (13) and (15), it is easy to see that the relative order of all the lengths in the system is

$$\delta \simeq \mathcal{L} \gg L/N = \mathcal{L}^{3/4}(R\ln\mathcal{N})^{1/4} \gg x = \mathcal{L}^{1/2}(R\ln\mathcal{N})^{1/2} \gg R\ln\mathcal{N} \gg R. \tag{18}$$

This order is consistent with the assumptions we started with.

As we saw above, the two last logarithmic terms in Eq. (12) are negligible. Therefore, the main driving force behind PECI is the gain in the self-energy of a sphere when the PE winds around it reducing its net charge. It is the difference between the left-hand side and the second term of Eq. (12). In other words, the sum of the self-energies $q^{*2}/2RD$ decreases when the PE distributes itself over a larger number of spheres. This correlation effect overcomes the macroscopic energy cost of overcharging the PE [the first term on the right-hand side of Eq. (12)]. Therefore, the PECI can be well obtained in the approximation where PE charge is smeared on the surface of spheres.[5,6]

Let us explain why we still call PECI calculated here a correlation effect. As we saw above the reason for this PECI is that each sphere is bound to several turns of a negatively charged PE. These turns can be considered as a correlation hole in the sense that this is the part of the PE, which interacts almost exclusively with the given sphere (other spheres are at much larger distance $x \gg R$). The segments of the PE wound around each sphere have the same length, $L/N - x \sim L/N \gg x$. Therefore, similarly to Refs. 10–13 we are dealing with Wigner-crystal-like correlations and the wound segment can be considered as a Wigner–Seitz cell of the bare sphere. The gain in the sphere self-energy mentioned above is nothing but the usual binding energy per sphere of a Wigner crystal (the interaction of a sphere with its Wigner–Seitz cell).

Note that because most of the PE length is wound around the spheres, the periodicity of positions of spheres covered by PE solenoids in the real space (see Fig. 1) is less important than in the case of a rigid PE (see Sec. VII) or other cases of charge inversion of rigid macroions by multivalent counterions.[11–13] Linkers between different pairs of neighboring spheres may differ in their length without a substantial change in the two major contributions to the free energy discussed above (the sphere self-energy gain and the macroscopic charging energy). The thermal motion can even melt the Wigner crystal of spheres in the real space while the length of the wound segment remains unchanged. Therefore the PECI is much more robust than the Wigner crystal in the real space.

IV. HIGH CONCENTRATION OF THE POLYELECTROLYTE: WEAK SCREENING CASE

In this section, we deal with the case when $n_p > n_s/N_0$ and there is shortage of spheres, each PE cannot get the optimal number, N_0, of spheres found in previous section. In this case, the number of spheres per PE is fixed: $N = n_s/n_p$. Therefore,

$$\frac{Q^*}{Q} = \frac{Q - n_s q/n_p}{Q} = 1 - \frac{n_{pi}}{n_p} = \frac{\delta}{\mathcal{L}}, \tag{19}$$

so that the PECI becomes weaker and linearly decreases with $n_p - n_{pi}$ as n_p grows. When n_p increases beyond the isoelectric point $n_{pi} = n_s q/Q$, the total charge of the complex Q^* is negative. The ratio Q^*/Q increases linearly from zero and eventually saturates at unity as n_p increases further. The behavior of Q^*/Q as function of n_p is plotted by the solid curve in Fig. 2.

Let us now discuss the behavior of the net charge of the sphere $q^* = \eta(\delta + x)$ as n_p increases. To do so, one has to solve Eq. (10) and find the distance x by which the spheres are separated along the PE. [We stress again that we are interested in the complex far enough from the isoelectric point, so that $x \gg R$ and Eq. (10) is valid.]

As n_p increases beyond n_s/N_0, the last two logarithmic terms in Eq. (10) are still negligible compare to the second term. Therefore, x is given by Eq. (13) [it should be noted that, here, $\delta = \mathcal{L}(1 - n_p/n_{pi})$ is a given length]. Correspondingly, q^* decreases linearly with δ.

As n_p moves closer to the isoelectric point, the net charge $q^* = \eta(\delta + x)$ decreases. When

$$\delta < \delta_c = R \ln \frac{L/N - x}{R} \simeq R \ln(\mathcal{L}/R), \tag{20}$$

[here, we replace $\ln((L/N-x)/R)$ by $\ln(\mathcal{L}/R)$ because near the isoelectric point, $\delta, x \ll \mathcal{L} \sim L/N$] the fourth and the first terms of Eq. (10) start to dominate over the second and third terms. This gives

$$x \simeq |\delta| \sqrt{\frac{\ln \mathcal{N}}{\ln(\mathcal{L}/R)}}. \tag{21}$$

Of course, Eqs. (13) and (21) match each other at $\delta = \delta_c$. To continue, let us consider the two important limiting cases $\ln \mathcal{N} \ll \ln(\mathcal{L}/R)$ and $\ln \mathcal{N} \gg \ln(\mathcal{L}/R)$.

A. The case $\ln \mathcal{N} \ll \ln(\mathcal{L}/R)$

In this case, $x \ll |\delta|$ and, therefore, the charge of a sphere $\eta(\delta + x)$, decreases to zero and becomes negative as n_p passes through n_{pi} (see Fig. 2). At $n_p > n_{pi}$, this SCI is driven by the fourth term of Eq. (10); the correlation energy of PE segment at the surface of the spheres. The charge inversion ratio $\mathcal{S} = |\delta + x|/\mathcal{L} \simeq |1 - n_p/n_{pi}|$ (see Fig. 2).

As n_p increases further, the charge of the sphere $\delta + x$ grows and the second and the fourth terms of Eq. (10) become the dominant ones. This gives

$$q^*/\eta = \delta + x = -R \ln \frac{L/N - x}{R} \simeq -R \ln \frac{\mathcal{L}}{R}, \tag{22}$$

so that the charge inversion ratio reaches its maximal possible value (see Fig. 2) which is equal to that for the complexation of a single sphere and a polyelectrolyte,[10]

$$\mathcal{S} = \frac{-q^*}{q} \simeq \frac{R}{\mathcal{L}} \ln \frac{\mathcal{L}}{R}.$$

Therefore, roughly speaking, it is inversely proportional to the number of turns of the PE around the sphere.

As n_p continues to increase, x increases and the third term of Eq. (10) becomes important making the sphere charge less negative. When $x > \mathcal{L}$, the second and third terms of Eq. (10) dominate. This gives

$$q^*/\eta = \delta + x = R \ln \frac{x}{R} \simeq R \ln \frac{L}{NR}, \tag{23}$$

so that the the net charge of the sphere changes sign from negative back to positive (not shown in Fig. 2). However, the condition of low salt solution, $x < r_D$, assumed in the derivation of Eq. (10), makes this re-entrant inversion of charge unrealistic. In a practical situation, $r_D < \mathcal{L}$ so that the necklace remains in the SCI range. A detailed consideration of the strong screening case $r_D < x$ is presented in the next section.

B. The case $\ln \mathcal{N} \gg \ln(\mathcal{L}/R)$

In this case, Eq. (21) gives $x \gg |\delta|$ and the charge of a sphere $\eta(\delta + x)$ touches zero but stays positive as n_p passes through the isoelectric point despite the fact that the total charge of the complex $Q^* = N\delta$ changes from positive to negative. This is because for a long PE, the macroscopic energy is very large and the complex is under a strong stress to increase x in order to reduce this macroscopic energy. This decreases the amount of the PE that can wind around each sphere making the sphere positive.

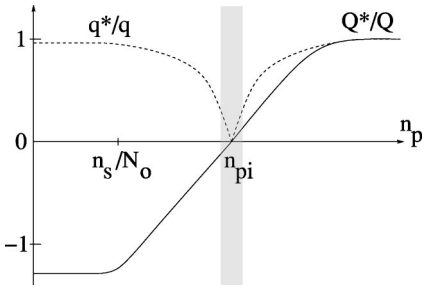

FIG. 4. Schematic plot of q^*/q and Q^*/Q as functions of PE concentration at a fixed and large sphere concentration n_s for the case B, Sec. IV. There is no SCI in this case. The shaded stripe shows the range of n_p around n_{pi} where condensation of PE molecules happens.

As n_p increases beyond the isoelectric point, $|\delta|$, x and the net charge $q^* = \delta + x$ of each sphere increase as well. Eventually $q^* \simeq q$, the PE unwinds from all of its spheres and becomes a straight rod to which N spheres are attached to. Substituting $x = L/N$ into Eq. (10) and neglecting the last two terms of this equation, one can estimate the value L/N at which PE unwinds from the spheres: $L/N \simeq \mathcal{L}(1 + \sqrt{\mathcal{L}/R \ln \mathcal{N}})$. As n_p increases further, q^*/q saturates at unity. The behavior of q^*/q as the function of n_p is depicted by the dashed line in Fig. 4.

We would like to emphasize that the inequality $R \ln \mathcal{N} \gg \ln(\mathcal{L}/R)$ may require unreasonably large screening radius r_D, so that the behavior presented in Fig. 2 for case A of this section is more generic.

V. CONDENSATION OF POLYELECTROLYTE-SPHERES COMPLEXES NEAR THE ISOELECTRIC POINT

Now, let us discuss properties of the system near the isoelectric point. Exactly at the isoelectric point $n_p = n_{pi}$, the spheres-PE complex is neutral, $Q^* = q^* = \delta = x = 0$ and $L/N = \mathcal{L}$. From Eq. (7) one gets the energy of one complex as $L \ln(A/a)$. It is the self-energy of the PE $L \ln(R/a)$ (the PE is straight up to distance R) plus the correlation energy $-L \ln(R/A)$ gained by arranging the PE turns into the one-dimensional Wigner crystal at the sphere surface [see the

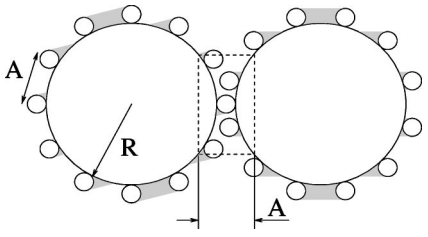

FIG. 5. Cross section through the centers of two touching spheres with worm like (gray) PE wound around them. At the place where two spheres touch each other (the region bounded by the broken line) the density of the PE and the background surface charge doubles which in turn leads to a gain in the correlation energy of PE segments. Near the isoelectric point, this gain is responsible for the condensation of spheres-PE complexes, forming a large neutral bundle of PE-spheres complexes.

discussion after Eq. (10)]. A consequence of this interpretation for the energy is that at the isoelectric point PE molecules condense onto each other forming a macroscopic neutral bundle. This is because the density of PE in the region where the spheres touch each other (the region bounded by broken line in Fig. 5) is doubled. Thus, the distance between PE segments, A_t, is halved, $A_t = A/2$, which results in a gain in the correlation energy. Simple geometrical calculation shows that this region has the area AR. Therefore, the PE in this region has total length R. The correlation energy gain per unit volume is

$$\Delta E_{\rm corr} \sim -\frac{n_p L}{\mathcal{L}} R \ln \frac{A}{A_t} \sim -\frac{n_p L}{\mathcal{L}} R.$$

Because of this finite gain in the correlation energy, there is a finite range of n_p around n_{pi} that the PE molecules are still in a condensed state. Let us try to find the width of this region.

To find the boundary of the condensation region on the left side of the isoelectric point ($n_p < n_{pi}$), one needs to compare the total energy of the system in the condensed and dissolved states. Here, the condensed state contains a macroscopic neutral bundle of PE-spheres complexes and ($n_s - n_p L/\mathcal{L}$) leftover spheres per unit volume. The bundle is neutral because charging a macroscopic body costs a lot of energy. The dissolved state is a solution of n_p isolated PE-spheres complexes per unit volume, each PE adsorbing n_s/n_p spheres. At the condensation concentration $n_p = n_{pl}$, we have to balance the correlation energy gain $\Delta E_{\rm corr}$ with the lost in the self-energy of ($n_s - n_p L/\mathcal{L}$) leftover spheres when they change from almost-neutralized spheres at the PE molecules to bare spheres in solution. Therefore the equation for the condensation point $n_p = n_{pl}$ is

$$\frac{n_{pl} L}{\mathcal{L}} R = \left(n_s - \frac{n_{pl} L}{\mathcal{L}} \right) \frac{\mathcal{L}^2}{2R} \tag{24}$$

or

$$1 - \frac{n_{pl}}{n_{pi}} \simeq \frac{R^2}{\mathcal{L}^2}. \tag{25}$$

On the right-hand side of the isoelectric point ($n_p > n_{pi}$), the condensed state is a macroscopic neutral bundle of PE and spheres and ($n_p - n_{pi}$) leftover bare PE molecules. $\Delta E_{\rm corr}$ needs to be balanced with the loss in the self-energy of PE molecules when they change from an almost-neutralized state to a bare state in solution. This gives for the resolubilization concentration n_{pr},

$$\frac{n_{pi} L}{\mathcal{L}} R = (n_{pr} - n_{pi}) L \ln \frac{r_D}{a} \tag{26}$$

or

$$\frac{n_{pr}}{n_{pi}} - 1 \simeq \frac{R}{\mathcal{L} \ln(r_D/a)}. \tag{27}$$

Finally, the total width of the region, $\Delta n_p = n_{pr} - n_{pl}$, around n_{pi} where condensation occurs is

$$\frac{\Delta n_p}{n_{pi}} = \frac{R^2}{\mathcal{L}^2} + \frac{R}{\mathcal{L} \ln(r_D/a)} \simeq \frac{R}{\mathcal{L} \ln(r_D/a)}. \tag{28}$$

Comparing this with Eq. (20), we see that the width of the condensation region is small, well within the region where the correlation energy [the fourth term in Eq. (10)] is important in determining conformation of the system. Therefore, in this range $\Delta E_{\rm corr}$ indeed dominates all other energies in Eq. (7) as we assumed.

VI. STRONG SCREENING BY THE MONOVALENT SALT

Until now, we assumed the salt concentration is small enough so that the screening radius r_D is larger than the distance between neighboring spheres, x. In the case of higher salt concentration when $r_D \ll x$, our theory needs some modifications. First, the macroscopic energy term [the first term in Eq. (4)] has to be replaced by the sum of repulsion energies of neighboring spheres. When $R \ll r_D \ll x$, it still has the form of interaction of two pointlike charges,

$$F(N,x) = N \frac{q^{*2}}{x + 2R} e^{-(x+2R)/r_D} + N f(x). \tag{29}$$

At the same time, all the logarithmic factors in Eq. (5) for $f(x)$ are cut off at r_D instead of x. Correspondingly, Eq. (10) [which is the result of the minimization of $F(N,x)$ with respect to x at a given N] should be replaced by

$$\frac{\partial F}{\partial x} = -\frac{(\delta + x)^2}{x r_D} e^{-x/r_D} + \frac{\delta + x}{R} - \ln \frac{r_D}{R} + \ln \frac{L/N - x}{R} = 0. \tag{30}$$

Let us concentrate on the PECI regime when $n_p < n_s/N_0$. In this case, the last two logarithmic terms in Eq. (30) can be neglected. This gives

$$x = r_D \ln \frac{(\delta + x) R}{r_D x} \simeq r_D \ln \frac{\mathcal{L} R}{r_D^2}. \tag{31}$$

Thus, the condition $r_D \ll x$ is equivalent to $r_D < \sqrt{\mathcal{L} R}$. In this case, $r_D \ll x \ll \delta \sim \mathcal{L}$. One can see that x only weakly depends on the number N of spheres attached to the PE. This is because the macroscopic self-energy of the complex which forces the PE to unwind from the sphere is strongly screened and diminished at distances beyond $r_D \ll x$.

Substituting Eq. (31) back into Eq. (29) and optimizing $F(N, x(N))$ with respect to N, we have, to the leading term

$$\frac{(L/N)^2}{2R} = \frac{r_D(\delta + x + 2L/N)}{R} + \frac{\mathcal{L} x}{R}, \tag{32}$$

so that

$$\frac{L}{N} = \sqrt{\mathcal{L} x} = \sqrt{\mathcal{L} r_D \ln \frac{\mathcal{L} R}{r_D^2}} \tag{33}$$

and the charge inversion ratio is

$$\mathcal{P} = \frac{N\delta}{L} = \sqrt{\frac{\mathcal{L}/r_D}{\ln(\mathcal{L} R/r_D^2)}}. \tag{34}$$

Comparing these results with those of Sec. III we see that due to screening, the spheres are closer to each other ($x \propto r_D$ instead of $\mathcal{L}^{1/2} R^{1/2}$) and a smaller length of the PE is wound around a sphere. In other words, the positive net charge of each sphere is larger ($L/N \propto \mathcal{L}^{1/2} r_D^{1/2}$ instead of $\mathcal{L}^{3/4} R^{1/4}$). Therefore, more spheres are attached to the PE,

making charge inversion much stronger ($\mathcal{P}\propto\mathcal{L}^{1/2}$ instead of $\mathcal{L}^{1/4}$). At the same time, when r_D increases to about $\sqrt{\mathcal{L}R}$, $x\sim r_D$, $L/N\simeq\mathcal{L}^{3/4}R^{1/4}$, $\mathcal{P}\simeq(\mathcal{L}/R)^{1/4}$ and we come back to the weak screening case.

It should be stressed that, for optimization with respect to x, the gain in a sphere's self-energy when PE winds around the sphere [the second term on the right-hand side of Eq. (30)] is balanced with the repulsion from its neighboring spheres (the first term). However, when determining N and $\mathcal{P}$ from Eq. (32), the repulsion between the spheres described by the first term on the right-hand side, which is of the order $\mathcal{L}r_D/R$, is negligible compared to the second term $\mathcal{L}x/R$. This term originates from the fact that when one brings a sphere from solution to the PE, hence gains the self-energy $(L/N)^2/2R$, the PE unwinds from other spheres in order to prepare the linker x for this new sphere.

Let us now consider even smaller screening radius $r_D \ll R$. In this case, one has to modify all the energy terms of Eq. (29). The self-energy of each sphere becomes $q^{*2}r_D/2R^2$ instead of $q^{*2}/2R$ and the interaction between neighboring spheres is

$$\frac{(q^*r_D^2/R^2)^2}{x}e^{-x/r_D}.$$

As a result, the minimization with respect to x gives

$$x=r_D\ln\frac{(\delta+x)r_D^2}{xR^2}\simeq r_D\ln\frac{\mathcal{L}r_D}{R^2}. \tag{35}$$

Now, an equation similar to Eq. (32) gives

$$\frac{L}{N}=\sqrt{\mathcal{L}x}=\sqrt{\mathcal{L}r_D\ln\frac{\mathcal{L}r_D}{R^2}} \tag{36}$$

and

$$\mathcal{P}=\frac{N\delta}{L}=\sqrt{\frac{\mathcal{L}/r_D}{\ln(\mathcal{L}r_D/R^2)}}, \tag{37}$$

so that the charge inversion is indeed stronger in this case and increases even faster than Eq. (34) with decreasing r_D. Equations (34) and (37) match each other when $r_D\sim R$. Equation (2) is their combination.

When the screening length becomes smaller than $R^2/\mathcal{L}$, the logarithmic factor $\ln(\mathcal{L}r_D/R^2)$ should be replaced by unity and Eqs. (35) and (36) give $L/N\sim R$ and $x\ll R$. This means that the PE is a straight rod with the bare spheres closely packed on it. The number of spheres attached to the PE reaches its maximal possible value $N=N_{\max}=L/R$, and so does the charge inversion ratio $\mathcal{P}=\mathcal{P}_{\max}=\mathcal{L}/R$. The behavior of $\mathcal{P}$ as a function of the screening length r_D is shown by the solid line in Fig. 6.

It should be noted that at very small value of the screening length, when the energy of interaction between a sphere and the PE is less than k_BT, the spheres detach from the PE and $\mathcal{P}$ rapidly decreases to zero.

Until now we have concentrated on the effect of strong screening on the optimal configuration of the PE-spheres complex at small concentration $n_p<n_s/N_0$, when spheres are in abundance. Now we want to discuss the role of screening in the opposite case, $n_p>n_s/N_0$. In this case, the number

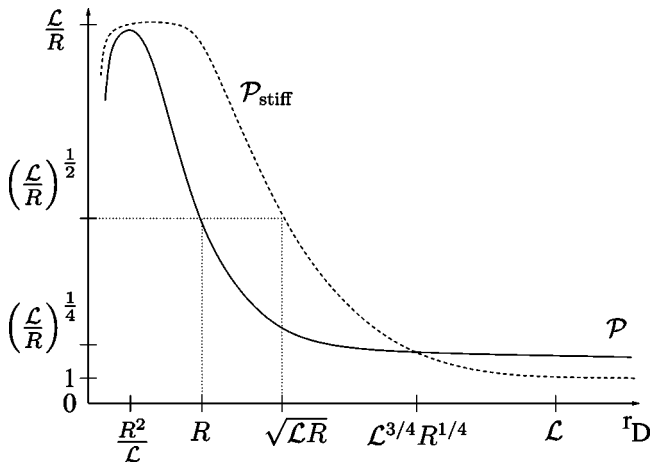

FIG. 6. Schematic plot of the charge inversion ratios $\mathcal{P}$ (the solid line) and $\mathcal{P}_{\text{stiff}}$ (the dashed line) as a function of screening length r_D. $\mathcal{P}_{\text{stiff}}>\mathcal{P}$ at $r_D\ll\mathcal{L}^{3/4}R^{1/4}$. $\mathcal{P}$ saturates when $r_D\sim R^2/\mathcal{L}$ while $\mathcal{P}_{\text{stiff}}$ saturates when $r_D\sim R$. For the definition of $\mathcal{P}_{\text{stiff}}$, see Sec. VII.

of spheres per PE $N=n_s/n_p$ is fixed and Eq. (19) remains valid (screening does not affect Q^*, because in any case all spheres are adsorbed by the PE). Qualitatively, Fig. 2 remains valid in this case. The length x is now given by the first equality of Eq. (31) for $r_D>R$ and by Eq. (35) for $r_D<R$ (the second equalities in these equations is not valid because δ is a given length). Therefore, x decreases as δ decreases.

In the case $r_D>R$, when δ decreases below r_D^2/R, Eq. (31) gives $x\leqslant r_D$ and we come back to the weak screening case described in Sec. IV, case A. All discussion about SCI and condensation of complexes in Sec. IV, case A remains valid in this case.

On the other hand, in the case $A<r_D<R$, our theory needs some correction. The value of δ below which the correlation energy between PE turns at the surface of a sphere is important is given by

$$\delta<\frac{R^2}{r_D}\ln\frac{L/N-x}{R}\simeq\frac{R^2}{r_D}\ln(\mathcal{L}/R), \tag{38}$$

instead of Eq. (20). This is because, in this case, the second term in Eq. (10) is $(\delta+x)r_D/R^2$ instead of $(\delta+x)/R$.

At the same time, the SCI effect at $n_p>n_{pi}$ is strongly enhanced in a way similar to the case of one sphere.[10] This is because the charging energy cost for SCI is strongly suppressed at small r_D while the short-range correlation energy between PE turns responsible for SCI remains unaffected. At small screening length, $\mathcal{S}$ can be larger than unity.

Strong screening ($A\ll r_D\ll R$) also affects the range of n_p where PE molecules form a neutral macroscopic bundle. When $r_D\ll R$, the self-energy cost $\mathcal{L}^2/2R$ in the right-hand side of Eq. (24) has to be replaced by $\mathcal{L}^2r_D/R^2$ per sphere while the short-range correlation energy on the left-hand side remains unaffected. This increases the width of this region to

$$\frac{\Delta n_p}{n_{pi}}\sim\frac{R^3}{\mathcal{L}^2r_D}+\frac{R}{\mathcal{L}\ln(r_D/a)}. \tag{39}$$

This width continue to grow with decreasing r_D. When $r_D \sim R^2/\mathcal{L} \sim A$, $R^3/\mathcal{L}^2 r_D \sim R/\mathcal{L}$ and the width more than doubles. When $r_D < A$, one can neglect the second term of Eq. (39) and arrive at Eq. (3). This equation predicts a strong growth of $\Delta n_p/n_{pi}$ with decreasing r_D, in qualitative agreement with experimental results of Ref. 1. It should be noted again that, as one see from comparison with Eq. (38), this coaservation range is well within the region of δ where the correlation energy between PE turns is the dominant energy term.

Finally, when $n_p \gg n_{pi}$, there is very small number of spheres per PE such that the length of the PE linker between them is larger than the optimal x given by Eqs. (31) and (35), the linker is no longer straight and each sphere with PE wound around it behaves independent from each other. SCI saturates at that given for the case of one sphere—one PE complexation.[10]

VII. POLYELECTROLYTE WITH EXTREMELY LARGE PERSISTENCE LENGTH

In this section we assume that the PE has an extremely large persistence length such that it cannot wind around a sphere. In this case, the PE is a straight rod to which the spheres are attached to. We are interested in the PECI regime where the concentration of spheres is large.

For a rodlike PE, $x = L/N$, $Nx' = -L/N = -x$, $\delta + x = \mathcal{L}$. In the case of weak screening, $r_D \gg L/N$, Eq. (12) can be rewritten as

$$\mathcal{L}\frac{N\delta}{L}\ln\mathcal{N} \simeq \mathcal{L}\ln\frac{L/2N}{R}. \tag{40}$$

The physical meaning of this equation is very simple: the left-hand side is the macroscopic charging energy cost when a sphere is brought from the bulk solution to the PE. The right-hand side is the gain in the correlation energy of the Wigner crystal of spheres along the PE which helps to overcome the charging energy cost. This correlation energy is the interaction of the sphere with two PE tails of length $L/2N$ which forms a Wigner–Seitz cell.

The charge inversion ratio can be easily calculated

$$\mathcal{P}_{\text{stiff}} = \frac{N\delta}{L} = \frac{\ln(L/2NR)}{\ln\mathcal{N}} \simeq \frac{\ln(\mathcal{L}/R)}{\ln\mathcal{N}}. \tag{41}$$

In the case of strong screening, $r_D \ll L/N$, the macroscopic charging energy cost should be replaced by the repulsion between neighboring spheres. At the same time, the logarithmic term in the expression for the correlation energy of the Wigner crystal of spheres along the PE should be cut off at r_D instead of L/N. Equation (40) now reads

$$\frac{\mathcal{L}^2}{r_D} e^{-L/Nr_D} = \mathcal{L}\ln\frac{r_D}{R}, \tag{42}$$

which gives $L/N \simeq r_D \ln(\mathcal{L}/r_D)$, and the charge inversion ratio

$$\mathcal{P}_{\text{stiff}} = \frac{N\delta}{L} \simeq \frac{\mathcal{L}}{r_D \ln(\mathcal{L}/r_D)} \gg 1. \tag{43}$$

Let us now compare these results with those for an intrinsically flexible PE case studied in Sec. III (weak screening) and Sec. V (strong screening).

At weak screening (Sec. III) $r_D > \mathcal{L} > R\ln\mathcal{N}$, Eqs. (17) and (41) give

$$\frac{\mathcal{P}_{\text{stiff}}}{\mathcal{P}} = \frac{R\ln(\mathcal{L}/R)}{\mathcal{L}^{1/4}(R\ln\mathcal{N})^{3/4}} \simeq \frac{\ln(\mathcal{L}/R)}{(\mathcal{L}/R)^{1/4}(\ln\mathcal{N})^{3/4}} \ll 1.$$

The last inequality is due to $\mathcal{L}/R \gg 1$ and $\ln\mathcal{N} \gg 1$.

As r_D decreases further so that $\mathcal{L} > r_D > \sqrt{\mathcal{L}R}$ we enter the strong screening regime for the rodlike PE but still stay in the weak screening regime for flexible PE. Using Eq. (43) for $\mathcal{P}_{\text{stiff}}$ and Eq. (17) for $\mathcal{P}$, we can easily see that the charge inversion for the rodlike PE starts to become stronger than charge inversion for the flexible PE when $r_D \sim \mathcal{L}^{3/4}R^{1/4}$.

When r_D continues to decrease in the range $r_D < \sqrt{\mathcal{L}R}$, we are in the strong screening regime for both types of PE. Equations (34) and (37) show that $\mathcal{P}$ is of the order of $\sqrt{\mathcal{L}/r_D}$ which is much smaller than $\mathcal{P}_{\text{stiff}} \simeq \mathcal{L}/r_D$.

The behavior of the charge inversion ratio as a function of r_D for the two types of PE is shown in Fig. 6. One can explore a transition from the flexible PE case to the stiff PE case by applying an external stretching force to the PE.[21] To describe this phenomenon, one has to add to the free energy (7) of the complex an additional term $-\mathcal{F}N(x+2R)$, where $\mathcal{F}$ is the external force. This new term is linearly proportional to the length of the spheres-PE complex. It adds a negative term $-\mathcal{F}$ to the right-hand side of Eq. (10) and therefore increases x. One then can proceed in exactly the same way as in Sec. III to find the conformation of the complex. At weak screening when $r_D \gg \mathcal{L}^{3/4}R^{1/4}$ (Sec. III), it is not difficult to show that x increases linearly with the strength of the external force when this force is small. At the same time, N_0 decreases linearly with $\mathcal{F}$ so that one by one, the spheres leave the PE as the force increases and PECI becomes weaker. When $\mathcal{F} \sim (\eta^2/D)(\mathcal{L}/R - \ln\mathcal{N})$ (so that the force helps to balance the attractive potential of the sphere with the macroscopic repulsive potential of the complex), one obtains $x \sim L/N$ and the PE unwinds completely from the spheres and becomes straight. The problem of complexation of PE and spheres, then, becomes that of a stiff PE described at the beginning of the section. This sequential release of spheres is similar to the problem of stretching a PE necklace in poor solvent.[22]

The picture is completely reversed at the strong screening case when $r_D \ll \mathcal{L}^{3/4}R^{1/4}$. In this case, as one stretches the PE, the spheres come to the PE one by one and make the charge inversion stronger. The strength of the force at which PE unwinds completely from the spheres can be calculated in exactly the same way as in the weak screening case. In the strong screening case, however, the macroscopic repulsive potential of the complex is very small so that the external force has to overcome only the attractive potential of the sphere in order to unwind the PE molecule. Therefore, PE unwinds completely when $\mathcal{F} \sim \eta^2\mathcal{L}/RD$ for $r_D > R$ and $\mathcal{F} \sim \eta^2\mathcal{L}r_D/R^2D$ for $r_D < R$.

It would be interesting to verify experimentally that the spheres leave the PE at weak screening and condense on the

PE at strong screening when the PE undergoes an external stretching force.

VIII. CONCLUSION

In conclusion, we would like to discuss four most important approximations used in this papers. Let us start from the use of the Debye–Hückel linear theory to describe screening by monovalent salt. It is known that if a PE molecule or a sphere are charged strongly enough this linear approximation does not work and the nonlinear condensation of counterions takes place, which leads to a renormalization of their charge. For the case of a rodlike PE this phenomenon is known as the Onsager–Manning condensation.[23] It happens when the linear charge density of PE η is larger than $\eta_c = Dk_BT/e$, where k_B is the Boltzmann constant and T is the temperature. Correspondingly, Debye–Hückel theory used above is valid when $\eta < \eta_c$.

The condition for the absence of counterion condensation on the charged spheres is more complicated and involves the concentration of monovalent salt as well. It is known that if a sphere is charged strongly enough, its counterions condense onto its surface to reduce its charge to the universal critical value $q_c = D\,\mathrm{Re}\,k_BT\ln(c_s/c)$, where e is the elementary charge, $c_s \sim q_c/R^3e$ and c are the counterion concentrations at the sphere surface and in the bulk respectively.[24] The condensation on the spheres can be neglected if $q = \mathcal{L}\eta$ is less than q_c or

$$r_D > \mathrm{Re}^{\mathcal{L}\eta/R\eta_c}. \tag{44}$$

At small enough η (such that $\eta/\eta_c < R/\mathcal{L}$), this condition reduces to $r_D > R$.

When $r_D < R$, each sphere can be considered as a plane with surface charge density $q/4\pi R^2$ and it is also known that if r_D is small enough, a charged plane is linearly screened. Specifically, Eq. (73) of Ref. 13 shows that screening is linear if

$$r_D < Ae^{\eta_c/\eta} \sim \frac{R^2}{\mathcal{L}} e^{\eta_c/\eta}. \tag{45}$$

At small enough η [such that $\eta < \eta_c/\ln(\mathcal{L}/R)$], this condition reduces to $r_D < R$.

Thus our theory has a wide range of applicability. For a PE with

$$\eta < \eta_c R/\mathcal{L}, \tag{46}$$

it is applicable for any value of the screening length r_D. Remarkably, the same inequality for η also guarantees that no Onsager–Manning condensation occurs on the spheres-PE rodlike complex with the inverted linear charge density $\eta\mathcal{P}$, even though the magnitude of this inverted charge can be much larger than the bare charge of the PE ($\mathcal{P} \gg 1$). Indeed, as we already know, $\mathcal{L}/R$ is the maximal possible value for $\mathcal{P}$ (see Fig. 6) therefore Eq. (46) guarantees that $\eta\mathcal{P}$ is smaller than the Onsager–Manning critical linear charge density η_c.

On the other hand, our theory literally is not applicable to strongly charged PE such as double helix DNA or too strongly charged spheres. We do, however, believe that our main results are qualitatively applicable in this case with properly normalized charges of the spheres and PE. A more detail study of the condensation problem will be the subject of a future work.

The second approximation which we want to address here is the assumption that the PE is flexible. It is valid if the elastic energy of PE winding around a sphere is smaller than the Coulomb energy of complexation. This can be true even if the persistence length of the strongly screened PE is of the order of a sphere diameter or somewhat larger. For example, theoretical estimates show that even in the nucleosome bead, the rigidity of DNA plays a secondary role. We should emphasize here that we talk about the intrinsic persistence length, ignoring the well known Odijk–Skolnick–Fixman electrostatic enhancement of the persistence length, which can be very substantial for a free PE molecule in the solution with small concentration of salt.[25] The reason for this is that at the sphere surface the charge of the PE is screened by the sphere's positive charge and it is the intrinsic persistence length of the PE which determines whether the PE can wrap around a sphere. All electrostatic interactions are explicitly taken into account in the correlation picture considered.

If the PE intrinsic persistence length is much larger than R, the ground state of the complex can strongly differ from that in the flexible case. In Sec. VI we studied the extreme case when the persistence length of the PE is infinite and the PE is rodlike. There is a wide range of intermediate magnitudes of persistence length which is not studied here. In this range nontrivial starlike configurations become possible even for one sphere.[26] For many spheres one can imagine different kinds of structures. Near the isoelectric point, it can be a rodlike complex made of a PE solenoid densely stuffed by spheres. It can be a similar cylinder where PE is instead winding around spheres makes several parallel to the cylinder axis straight strands on the surface of the cylinder, which are connected by loops at the cylinder edges. This strands repel each other and form periodic in polar angle ''Wigner crystal.'' These and other possible configurations should be studied in future works.

The third simplification used in this paper was an assumption that the number and the size of spheres in the solution is fixed. When we try to compare this theory with the data on the micelles–PE system[1] we immediately see that, strictly speaking, this is a different problem, because in the experiment of Ref. 1 the amount of lipids is fixed, but the number and size of micelles is determined by equilibrium conditions and may depend, for example, on the screening radius of the solution. This complication should be taken into account by a future theory.

The fourth important assumption we made in this paper is that the concentration of spheres, in the solution, n_s, is large enough so that their entropy can be neglected. This assumption leads, for example, to the conclusion that in the case $n_p > n_s/N_0$, all the spheres are consumed by the PE. Actually, even in this case, there is a finite, but exponentially small concentration, n_{s0}, of free spheres in the solution next to PE because the binding energy of a sphere to PE is finite. In other words, this is the concentration of the ''saturated vapor'' of spheres right above the correlated liquid of spheres on the PE. When total concentration of spheres, n_s,

is so small that it is comparable to n_{s0} effect of free spheres becomes very important. For example, at such small n_s spheres fail to neutralize PE near isoelectric point. At the limit of $n_p \to 0$ neutralization happens at $n_s = n_{s0}$. Therefore, the plot of the line $n_s(n_p)$ at which neutralization takes place deviates from the isoelectric line $n_s = n_p L/\mathcal{L}$ at small n_p and n_s (see dashed line at Fig. 7). Correspondingly, the region of the condensation of PE-spheres complexes on the plane (n_s, n_p) looks as the shaded region shown in Fig. 7.

The theory of condensation at small n_p is similar to the theory of condensation of DNA by multivalent counterions at a small concentration of DNA.[17] Experimental data on re-entrant condensation of DNA have a qualitatively similar shape of the condensation domain.[27]

Summarizing our results, we have studied complexation of a negative PE with positive spherical macroions in salty water. Under solely the influence of electrostatic interactions, a PE molecule winding around individual spheres binds spheres in a beads-on-a-string structure. At a large sphere concentration, we found interesting phenomena on both sides of the isoelectric point, at which the total charge of all PE molecules is exactly compensated by total charge of spheres. When the PE concentration is below the isoelectric point, spheres overcharge the PE so that the net charge of the PE together with bound spheres is positive and can be substantially larger than the absolute value of the bare charge of the PE. When the PE concentration is above the isoelectric point, the net charge of the PE segment is not inverted, while the net charge of each sphere together with the PE winding around it becomes inverted and negative. It can be larger than the bare charge of the sphere if the screening radius of the solution is small enough.

In the narrow vicinity of the isoelectric point PE-spheres complexes condense together in bundles. We calculated the width of the range of the PE concentration where the condensation takes place and showed that it grows very fast with decreasing screening radius of the solution.

All these phenomena are results of repulsive correlations between PE turns on the surface of spheres and of the spheres on the PE, which cannot be included in any Poisson–Boltzmann-type description of the mutual screening of PE and spheres. The repulsive correlations between PE turns on spheres are responsible for charge inversion of individual spheres (SCI) and the condensation of PE-spheres complexes in bundles. In the latter case this phenomenon is illustrated by Fig. 5. In the former case, additional discussion of the physics of this phenomenon can be found in Ref. 10. Wigner-crystal-like correlations of turns mean that each turn is surrounded by a stripe of positively charge macroion surface, which can be considered as its positive correlation hole.

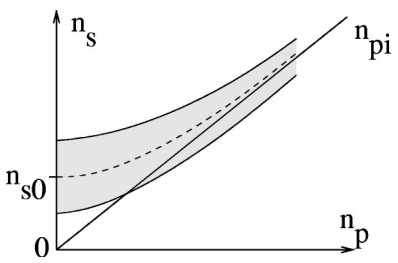

FIG. 7. Schematic phase diagram of the condensation of spheres-PE complexes in the (n_p, n_s)-plane for a very large PE length L. Complexes condense in the shaded domain. The straight line corresponds to the isoelectric point $n_s = n_p L/\mathcal{L}$. The dash line shows the function $n_s(n_p)$ at which an isolated PE-spheres complex is neutral.

The most interesting phenomenon of the inversion of charge of the PE (PECI) by a large number of adsorbed spheres is related to the fact that each sphere is bound to several turns of negatively charged PE. These turns can be considered as a correlation hole, because this is part of the PE, which almost exclusively interacts with the given sphere. In this sense, once more we are dealing with correlations. The segments of the PE wound around each sphere have the same length and they constitute most of the PE's total length. Therefore, these correlations are similar to Wigner-crystal-like correlations which are responsible for charge inversion of a rigid macroion.[10–13,15] This confirms our point of view that Wigner-crystal-like correlations are the universal driving force of charge inversion.

Our theory, with minor modifications, can also describe the complexation of polyelectrolytes with macroions of nonspherical shape. An example of such a system can be the complexation of two oppositely charged polyelectrolytes in water solution. Let us assume that the negative PE is long and flexible while the positive PE is shorter, stronger charged, and rigid. Then the negative PE molecule wraps around the positive one and the only change which should be made in our theory is to replace the expression for self-energy of charged sphere by the corresponding expression for charged rod. The case when the positive PE is flexible on the first glance seems to be more complicated. However, away from isoelectric point positive PE is overscreened or underscreened by the wrapping negative one so that it has a rodlike shape. Therefore, even in this case our theory is valid with the above-mentioned minor change.

ACKNOWLEDGMENTS

We are grateful to A. Yu. Grosberg for helpful discussions and reading of the manuscript. This work was supported by NSF DMR-9985985.

[1] Y. Wang, K. Kimura, Q. Huang, P. L. Dubin, and W. Jaeger, Macromolecules **32**, 7128 (1999).
[2] V. A. Kabanov, V. P. Evdakov, M. I. Mustafaev, and A. D. Antipina, Mol. Biol. (Moscow) **11**, 52 (1976); J. Xia and P. L. Dubin, in *Macromolecular Complexes in Chemistry and Biology*, edited by P. L. Dubin *et al.* (Springer-Verlag, Berlin, 1994).
[3] E. Braun, Y. Eichen, U. Sivan, and G. Ben-Yoseph, Nature (London) **391**, 775 (1998).
[4] T. Wallin and P. Linse, Langmuir **12**, 305 (1996).
[5] E. M. Mateescu, C. Jeppersen, and P. Pincus, Europhys. Lett. **46**, 454 (1999).
[6] S. Y. Park, R. F. Bruinsma, and W. M. Gelbart, Europhys. Lett. **46**, 493 (1999).
[7] R. R. Netz and J. F. Joanny, Macromolecules **32**, 9026 (1999).
[8] P. Sens and E. Gurovitch, Phys. Rev. Lett. **82**, 339 (1999).
[9] P. Chodanowski and S. Stoll, Macromolecules **34**, 333 (2001).
[10] T. T. Nguyen and B. I. Shklovskii, Physica A **293**, N3–4, 444 (2001).
[11] V. I. Perel and B. I. Shklovskii, Physica A **274**, 446 (1999); B. I. Shklovskii, Phys. Rev. E **60**, 5802 (1999).
[12] T. T. Nguyen, A. Yu. Grosberg, and B. I. Shklovskii, Phys. Rev. Lett. **85**, 1568 (2000).

[13] T. T. Nguyen, A. Yu. Grosberg, and B. I. Shklovskii, J. Chem. Phys. **113**, 1110 (2000).
[14] R. R. Netz and J. F. Joanny, Macromolecules **32**, 9013 (1999).
[15] A. V. Dobrynin, A. Deshkovski, and M. Rubinstein, Macromolecules **34**, 8888 (2001).
[16] I. Rouzina and V. A. Bloomfield, J. Phys. Chem. **100**, 9977 (1996); N. Gronbech-Jensen, R. J. Mashl, R. F. Bruinsma, and W. M. Gelbart, Phys. Rev. Lett. **78**, 2477 (1997); B. J. Ha and A. J. Liu, *ibid.* **79**, 1289 (1997); R. Podgornik and V. A. Parsegian, *ibid.* **80**, 1560 (1998); J. J. Arenzon, J. F. Stilck, and Y. Levin, cond-mat/9806358; B. I. Shklovskii, Phys. Rev. Lett. **82**, 3268 (1999).
[17] T. T. Nguyen, I. Rouzina, and B. I. Shklovskii, J. Chem. Phys. **112**, 2562 (2000).
[18] M. Jonsson and P. Linse, J. Chem. Phys. (submitted).
[19] J. O. Rädler, I. Koltover, T. Salditt, and C. R. Safinya, Science **275**, 810 (1997).
[20] R. F. Bruinsma, Eur. Phys. J. B **4**, 75 (1998).
[21] This idea was suggested to us by A. Yu. Grosberg.
[22] T. A. Vilgis, A. Johner, and J. F. Joanny, Eur. Phys. J. E **2**, 289 (2000); M. N. Tamashiro and H. Schiessel, Macromolecules **33**, 5263 (2000).
[23] G. S. Manning, J. Chem. Phys. **51**, 924 (1969).
[24] M. Guerom and G. Weisbuch, Biopolymers **19**, 353 (1980); S. Alexander, P. M. Chaikin, P. Grant, G. J. Morales, P. Pincus, and D. Hone, J. Chem. Phys. **80**, 5776 (1984); S. A. Safran, P. A. Pincus, M. E. Cates, and F. C. MacKintosh, J. Phys. (Paris) **51**, 503 (1990); L. Belloni, doctoral thesis, University of Paris IV, 1982; Chem. Phys. **99**, 43 (1985).
[25] T. Odijk, J. Polym. Sci., Polym. Chem. Ed. **15**, 477 (1977); J. Skolnick and M. Fixman, Macromolecules **10**, 5 (1977); **10**, 944 (1977).
[26] H. Schiessel, J. Rudnick, R. Bruinsma, and W. M. Gelbart, Europhys. Lett. **51**, 237 (2000).
[27] E. Raspaud, I. Chaperon, A. Leforestier, and F. Livolant, Biophys. J. **77**, 1547 (1999).